Laser-induced Writing of Submicron Surface Relief Gratings in Fused Silica on the Fly

Rico BÖHME, Klaus ZIMMER

Leibniz-Institut für Oberflächenmodifizierung e. V., Permoserstr. 15, 04318 Leipzig, Germany
E-mail: rico.boehme@iom-leipzig.de

The hybrid laser processing method LIBWE (*laser-induced backside wet etching*) allows the defined micro and submicron structuring of transparent materials like fused silica at small laser fluences and with high quality. In this study the etching of fused silica with mercury as liquid absorber is demonstrated using an excimer laser ($\lambda = 248$ nm, 25 ns pulses). The high absorption coefficient of liquid metals enlarges the absorption of the UV laser radiation so that despite the high reflectivity the threshold for etching was measured to be 0.75 J/cm². With rising laser fluence the etch rate linearly increases in the whole laser fluence range and reaches a value of 650 nm/pulse at a laser fluence of about 10 J/cm². For the etching of 2D periodic sub-micron structures into fused silica, four interfering laser beams were used generated by projection of a chessboard-like diffraction phase mask. In conjunction with liquid-metal LIBWE, submicron surface relief gratings with regular dot patterns have been realized on planar and prestructured samples in a one-step direct fabrication process. The large etch rates at LIBWE by means of the liquid metal enable a high-speed processing; gratings with a period of 800 nm and a depth up to 60 nm can be etched on the fly with only one laser pulse.

DOI: 10.2961/jlmn.2007.03.0003

Keywords: laser, backside etching, LIBWE, fused silica, liquid, metal, mercury, submicron gratings, periodic dot pattern

1. Introduction

Laser-induced backside wet etching (LIBWE) [1,2] is a recently devised processing technique that allows the precise etching of transparent materials by pulsed laser radiation with high accuracy. Usually, LIBWE makes use of an organic liquid (solvents or organic dye solutions) at the back surface of the transparent material that absorbs the laser beam and serves as a source for heating the solid material up to the melting or softening point. Subsequent secondary processes of thermal expansion, vaporization, bubble formation, film deposition, and shock wave generation are involved in the etching process, too. The influence of experimental parameters on etch rate, topography, incubation effects, and structural and chemical properties of etched surfaces were investigated for a number of transparent dielectric materials [1-13]. The etch mechanism actually under discussion is suggested as a sequence of surface heating by the hot laser-heated liquid, an increasing of the solid temperature up to a critical value (e. g. the softening or melting point) followed by mechanical removing of the softened or melted surface layer by the heated liquid together with shock waves on high pressure [1,13-15]. The etching is regularly accompanied by incubation effects [6,16] similar to laser ablation in air [17] with the results of instabilities of the etching at low fluences and pulse numbers, the increase of the etch rate during prolonged pulsed laser irradiation, and the reduction of the threshold fluence for etching with the number of applied laser pulses [6,18]. At LIBWE with hydrocarbon solutions one origin for the surface modification and consequently the incubation effects is the decomposition of the organic molecules. Due to the high laser-power-initialized pressure-, temperature-, and photon-induced fragmentation processes [19], the formation of a carbon modified layer [4,15,20] is caused that changes the physical/optical/chemical properties of the solid/liquid interface.

Recent results show the application of liquid metals such as gallium or mercury for etching instead of organic solvents or solutions [21-25]. Liquid-metal-LIBWE features negligible incubation effects, higher etching threshold fluences, and very large etch rates (30-600 nm/pulse) while the surface quality is as high as for hydrocarbon LIBWE. For the etching of periodic sub-micron structures on a solid surface, interfering laser beams are used generated by the projection of diffraction masks. In conjunction with the backside etching approach, submicron surface relief gratings with regular line patterns [5,26,27] can be realized on planar transparent samples in a one-step direct fabrication process employing organic liquids and hundreds of laser pulses. Otherwise, the large etch rates at liquid-metal-LIBWE enable a high-speed processing of deep submicron gratings with one laser pulse.

2. Experimental

The experimental set-up for LIBWE was described elsewhere [1,2]. A KrF excimer laser (λ = 248 nm, 10 Hz, τ_p = 25 ns) incorporated into a laser workstation has been used for the experiments presented. The etching chamber that holds the samples was attached to a computer controlled x-y-z stage. A reflective objective (Schwarzschild, 15 x demagnification) with an optical resolution of 1.5 µm was used once for projecting a square aperture with a size of 100 µm x 100 µm and further for the projection of the phase mask onto the sample back surface. In all investigations fused silica samples cut from double side polished wafers with a thickness of about 380 µm and a low surface roughness (< 0.3 nm rms) were used as received without additional cleaning. Pure mercury (Degussa, 99.999 %) was used as liquid absorber at room temperature.

The principal experimental set-up for the phase mask projection is shown in [26]. The zeroth order of the diffracted laser light was not allowed to interact with the sample due to the grating design and the optical set-up. In the actual experiments, a chessboard phase mask has been used. The first orders were deflected along the objective beam path and produce a four-beam-interference pattern at the back surface of the transparent sample. An aperture blocked out the second and higher orders. For quantification, the peak fluence (Φ_{Peak}) of the periodic intensity distribution of interference pattern has been determined by dividing the measured pulse energy (with joulemeter) by the size of the beam at the back surface (90 µm x 80 µm) multiplied by two.

After the etching process the samples were cleaned from the mercury first with a soft tissue and after that by selective etching of the mercury with diluted nitric acid. Finally the samples were ultrasonically cleaned with distilled water and acetone and were blown dry in a nitrogen stream. The depths of the etched pits were measured with a white light interference microscope (10 x and 50 x magnification). Atomic force microscopy (AFM) investigations were performed for grating examination and scanning electron microscopy (SEM) images were taken after deposition of a thin chromium film to the samples surfaces.

3. Results

Fig. 1 shows the etch rate and the efficiency of etching of fused silica with liquid mercury in dependence on the applied laser fluence. The etch depth is measured after 10 applied laser pulses, thus the shown etch rate presents an averaging over all pulses. In addition, the efficiency of etching per laser pulse and fluence (etch rate divided by laser fluence; right axis) is shown that gives the etched volume per energy unit. The etch rate rise seems to be almost linear with the laser fluence in the range between 1 and 10 J/cm². Otherwise, the increasing efficiency of etching betrays that for the fluences region below 2.5 J/cm², the etch rate rises stronger than proportional with the laser fluence (low fluence region). For larger fluences, the efficiency does not significantly differ and reveals etching in steady state similar to the middle fluence region by use of organic liquids [6]. The experimental threshold fluence - the smallest fluence at

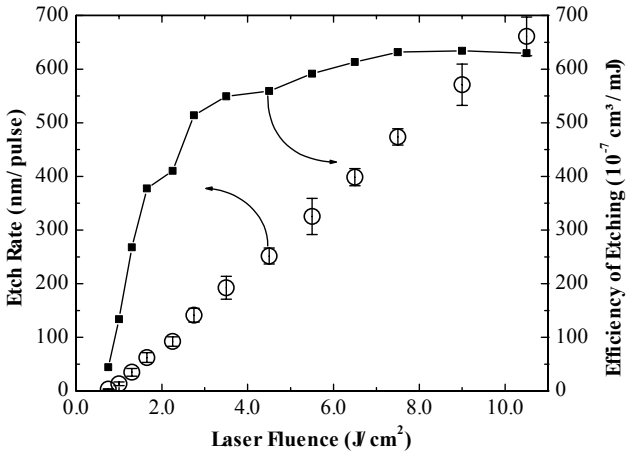

Fig. 1: Etch rate (left axis) and efficiency of etching (right axis) in dependence on the laser fluence. 10 laser pulses are applied with liquid metal mercury as absorbing liquid.

which after 10 pulses a measurable etching occurs - is determined to be 0.75 J/cm² which is more than one order of magnitude smaller than for direct laser ablation of fused silica in air (larger than 10 J/cm² [17]). This estimated threshold fluence is larger than the threshold fluences for LIBWE with hydrocarbon liquids or solutions ranging from 0.25 to 0.6 J/cm² whereby the exact value depends on the kind of the used solution but is much lower than the threshold fluence for LIBWE using gallium of 1.3 J/cm² [21]. But similar to LIBWE with gallium large etch rates (~ 600 nm/pulse) have been measured that exceed the etch rates attained with organic absorbers by more than 10 to 100 times (see Refs. cited in [14]).

By means of projecting the transmission phase mask, a periodic fluence distribution is generated onto the back surface of the fused silica sample and a 2D grating with a period of about 800 nm has been etched (Fig. 2). After the etching the fabricated topography features two main characteristics, the development of the expected relief gratings and a homogeneous material etching over the entire illuminated area, further called *over-all-etching* (OAE) [5]. The laser fluence affects the grating depth, the OAE depth, and the grating shape. Fig. 3 shows the grating depth after one laser pulse in dependence on the peak fluence. At small fluences (< 1.5 J/cm²) only shallow, but well defined, holes (Fig. 2a and b) can be etched. Here, the diameter of a single hole is about 300 nm. An optimum in grating depth (40 … 60 nm) and shape (deep, acute-angled holes Fig. 2c) can be found for exposures with 1.8 and 2.4 J/cm². With further increasing laser fluence, the amplitude of the gratings continuously decreases and the shape becomes a smooth 2D sinusoidal relief (Fig. 2d). For peak fluences larger than 4.7 J/cm², no periodic topography exists. At the same time, the OAE depth increases (Fig. 3). A similar decrease of the grating depth with increasing laser fluence for LIBWE with organic liquid was described in [5] and is probably related to a LIBWE inherent smoothing effect [5]. Comparing the received results of grating depths (Fig. 3) and shapes (Fig. 2) with the etch rates after homogeneous irradiation (Fig. 1) it becomes visible, that gratings with sufficiently high quality can be written into fused silica

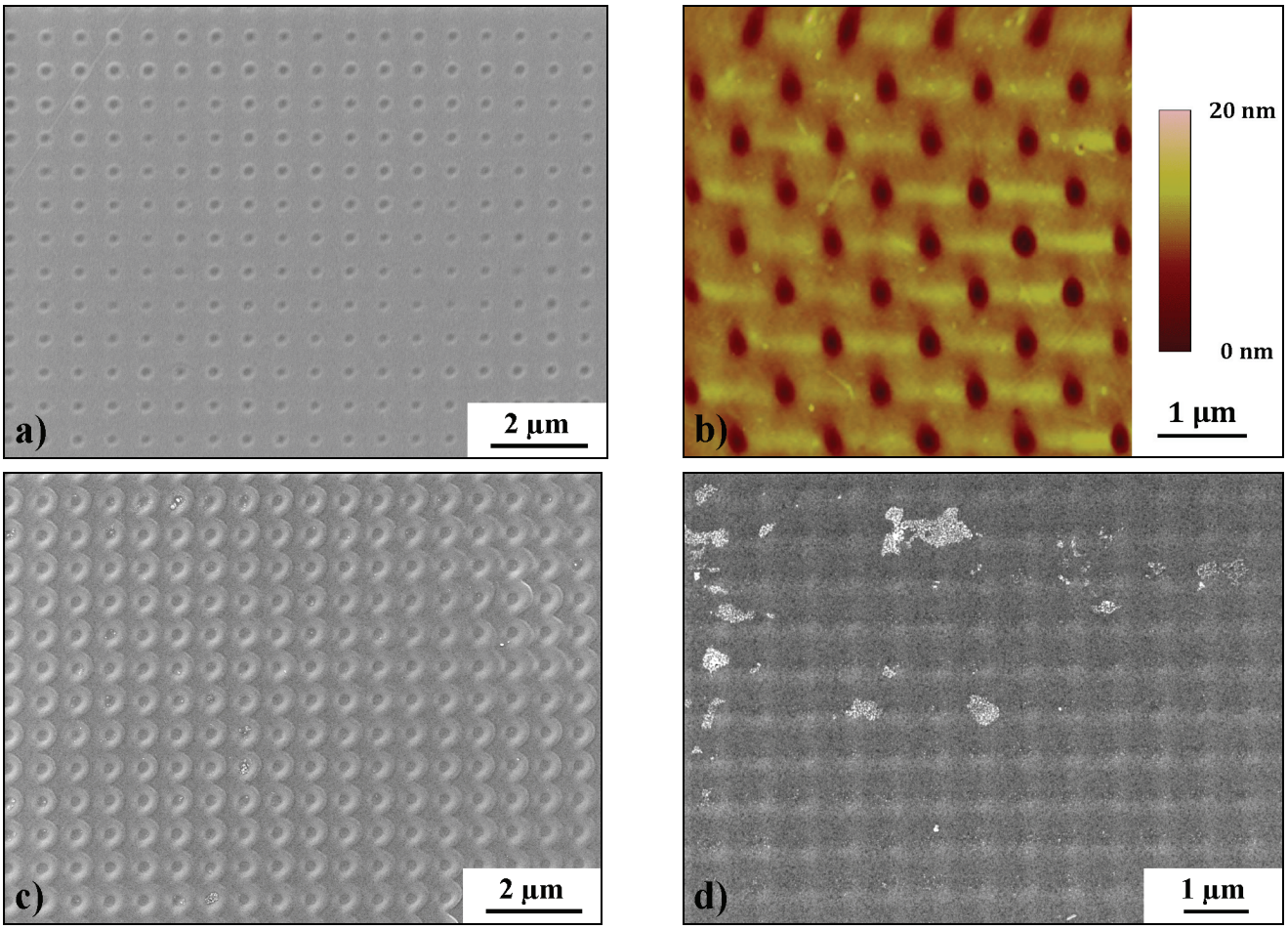

Fig. 2: Micrographs of etched 2D submicron relief gratings in fused silica recorded by SEM (a, c,d) and AFM (b). The dot patterns have been etched with mercury and one laser pulse for a) and b) Φ_{Peak} = 1.5 J/cm²; c) Φ_{Peak} = 1.8 J/cm²; d) Φ_{Peak} = 3.1 J/cm².

only in the low fluence region (< 2.5 J/cm²).

Fig. 4 shows the effect of the pulse number on the grating depth. The periodic patterns have been etched with different peak fluences. At Φ_{Peak} = 3.1 J/cm², the grating amplitude does not differ significantly between 1 and 30 laser pulses per place. For Φ_{Peak} = 1.5 J/cm², the depth increases from 10 nm (1 pulse) to 55 nm (30 pulses). At the optimized laser fluence for grating processing (Φ_{Peak} = 1.8 J/cm², see also Fig. 3), the amplitude of the gratings grows within 10 laser pulses, reaches its maximum of 160 nm at the 10th pulse, and starts to decrease with further growing pulse number. A similar behavior has been observed for the writing of gratings by both direct ablation [28] as well as LIBWE with organic liquids [5,27]. Such effect is usually associated with materials etching or ablation at the dark fringes of interference pattern due to slightly reduced contrast during the prolonged irradiation.

For application, the available size of the laser beam by means of phase mask projection and liquid-metal-LIBWE is too small (90 µm x 80 µm). As a solution, a step-and-repeat process has been realized to fabricate a

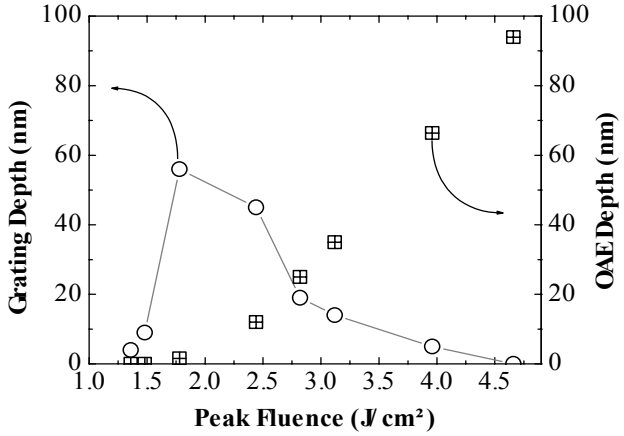

Fig. 3: Depths of 2D submicron gratings inscribed into fused silica with one laser pulse (left axis) and the simultaneously caused over-all-etching depth (right axis).

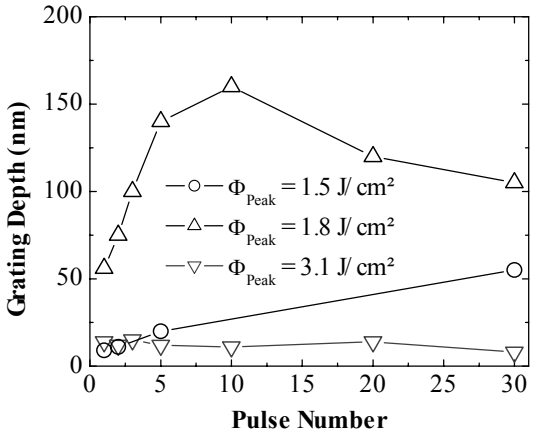

Fig. 4: Depths of 2D submicron gratings inscribed into fused silica as a function of the number of applied laser pulses. The gratings etched using different peak fluences.

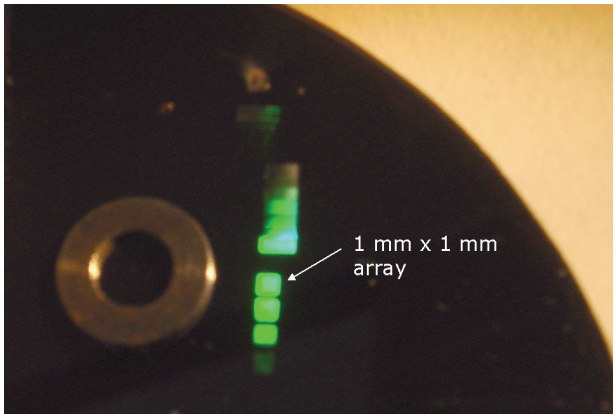

Fig. 5: Photograph of a fused silica sample with on-the-fly-written 2D dot patterns on large areas. For better visualization, the sample is coated with a 20 nm chromium layer and illuminated with white light from the right.

2D relief grating at an area of 1 mm x 1 mm (Fig. 5). In this experiment, the small spots including the grating are written on the fly (1 laser pulse per place) with a peak fluence of 1.8 J/cm².

Beside "simple" planar surfaces, the etching of relief gratings has been realized on curved fused silica surface in a one-step direct fabrication process, too. Fig. 6 presents an etched 2D grating onto a rectangular grating structure of 11 µm period and 4 µm depth. The 2D grating is etched with one laser pulse at Φ_{Peak} = 1.8 J/cm² simultaneously on the bottom and the top of the binary line grating without lost of contour (no rounding of the edges) and without moving the sample. The defined and high-resolution 2D surface relief gratings, the remaining precision of the primary curved surface contour, and the resulting overall low roughness confirm the capabilities of this laser etch technique.

5. Summary

The laser-induced backside wet etching of sub-micron 2D relief gratings into fused silica is demonstrated by using the liquid metal mercury as absorber. The fabricated dot patterns with a period of about 800 nm and a minimum hole diameter of 300 nm are very regular and homogeneous over the entire illuminated area. The large etch rates by means of liquid metals and the only marginal incubation effects qualify the presented method for the on-the-fly laser processing. Grating depths of about 60 nm can be achieved with one laser pulse and at small laser fluences. Due to the on-the-fly laser processing, arbitrarily large areas with the 2D relief gratings can be fabricated. In addition, gratings have been etched on a binary topography on the bottom and the top of the line grating without lost of contour. In summary, the laser-induced backside etching of fused silica with mercury by means of phase mask projection combines small etching threshold, high etch rates, and a still smooth etching of well defined patterns into material surfaces and enables a fast processing of high quality surface patterns.

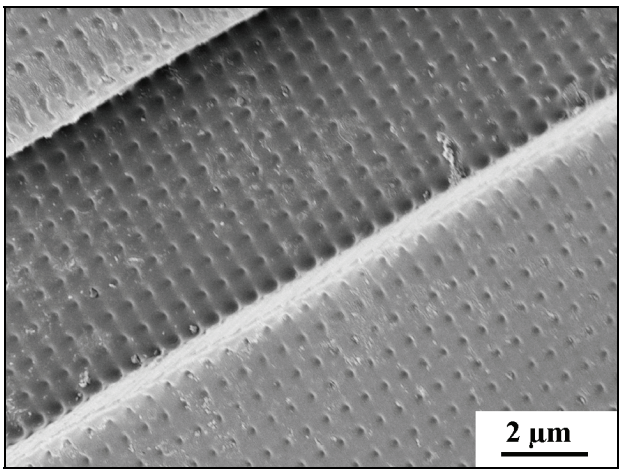

Fig. 6: SEM image of periodic dot patterns etched subsequently onto a pre-structured fused silica surface.

Acknowledgements

The authors are grateful to M. Mäder for her skilled SEM investigations and to Ph. Hadrava, U. Gleisberg and E. Salamatin for the help in the experimental work and performing the microscopy investigations. Parts of the work were financially support by the Deutsche Forschungsgemeinschaft Germany under contract DFG ZI660/3.

References

[1] J. Wang, H. Niino, and A. Yabe: Appl. Phys. A **68** (1), (1999) 111.
[2] R. Böhme, A. Braun, and K. Zimmer: Appl. Surf. Sci. **186** (1-4), (2002) 276.
[3] K. Zimmer, A. Braun, and R. Böhme: Appl. Surf. Sci. **208**, (2003) 199.
[4] R. Böhme, D. Spemann, and K. Zimmer: Thin Solid Films **453-454**, (2004) 127.
[5] R. Böhme, J. Zajadacz, K. Zimmer, and B. Rauschenbach: Appl. Phys. A **80**, (2005) 433.
[6] R. Böhme and K. Zimmer: Appl. Surf. Sci. **247**, (2005) 256.
[7] J. Wang, H. Niino, and A. Yabe: Appl. Phys. A **69**, (1999) 271.
[8] J. Wang, H. Niino, and A. Yabe: Jpn. J. Appl. Phys. **38** (7A), (1999) 761.
[9] X. M. Ding, T. Sato, Y. Kawaguchi, and H. Niino: Jpn. J. Appl. Phys. **42** (2B), (2003) 176.
[10] X. Ding, Y. Kawaguchi, T. Sato, A. Narazaki, R. Kurosaki, and H. Niino: J. Photochem. Photobiol. A **166** (1-3), (2004) 129.
[11] H. Niino, Y. Kawaguchi, T. Sato, A. Narazaki, T. Gumpenberger, and R. Kurosaki: Appl. Surf. Sci. **252**, (2006) 4387.
[12] G. Kopitkovas, T. Lippert, C. David, A. Wokaun, and J. Gobrecht: Thin Solid Films **453-454**, (2004) 31.
[13] C. Vass, T. Smausz, and B. Hopp: J. Phys. D **37** (17), (2004) 2449.
[14] Y. Kawaguchi, X. Ding, A. Narazaki, T. Sato, and H. Niino: Appl. Phys. A **80** (2), (2005) 275.
[15] G. Kopitkovas, T. Lippert, C. David, S. Canulescu, A. Wokaun, and J. Gobrecht: J. Photochem. Photobiol. A **166** (1-3), (2004) 135.
[16] Y. Yasui, H. Niino, Y. Kawaguchi, and A. Yabe: Appl. Surf. Sci. **186** (1-4), (2002) 552.
[17] J. Ihlemann and B. Wolff-Rottke: Appl. Surf. Sci. **106**, (1996) 282.

[18] R. Böhme and K. Zimmer: Journal of Physics D: Applied Physics **40** (10), (2007) 3060.
[19] J. Pola, M. Urbanova, Z. Bastl, Z. Plzak, J. Subrt, V. Vorlicek, I. Gregora, C. Crowley, and R. Taylor: Carbon **35** (5), (1997) 605.
[20] H. Niino, Y. Yasui, X. M. Ding, A. Narazaki, T. Sato, Y. Kawaguchi, and A. Yabe: J. Photochem. Photobiol. A **158** (2-3), (2003) 179.
[21] K. Zimmer, R. Böhme, D. Ruthe, and B. Rauschenbach: Appl. Phys. A **84**, (2006) 455.
[22] K. Zimmer, R. Böhme, S. Pissadakis, L. Hartwig, G. Reisse, and B. Rauschenbach: Appl. Surf. Sci. **253**, (2006) 2796.
[23] K. Zimmer, R. Böhme, D. Hirsch, and B. Rauschenbach: J. Phys. D **39**, (2006) 4651.
[24] K. Zimmer, R. Böhme, and B. Rauschenbach: Appl. Phys. A **86** (3), (2007) 409.
[25] R. Böhme and K. Zimmer: Appl. Surf. Sci. **253** (19), (2007) 8091.
[26] K. Zimmer, R. Böhme, A. Braun, B. Rauschenbach, and F. Bigl: Appl. Phys. A **74** (4), (2002) 453.
[27] S. Pissadakis, R. Böhme, and K. Zimmer: Optics Express **15** (4), (2007) 1428.
[28] S. Pissadakis, L. Reekie, M. Hempstead, M. N. Zervas, and J. S. Wilkinson: Appl. Phys. A **69**, (1999) S739.

(Received: April 24, 2007, Accepted: August 23, 2007)